Bio Inspired Aircraft Wing Design to Reduce Flow Generated Noise

S.S. Gunarathne
Department of Mechanical Engineering
Faculty of Engineering
University of Sri Jayewardenepura
Rathmalana, Sri Lanka
sulochanasgunarathne@gmail.com

D. Appuhamy
Department of Mechanical Engineering
Faculty of Engineering
University of Sri Jayewardenepura
Rathmalana, Sri Lanka
dinithika.appuhamy@sjp.ac.lk

G. Siriwardana
Department of Mechanical Engineering
Faculty of Engineering
University of Sri Jayewardenepura
Rathmalana, Sri Lanka
geethal@sjp.ac.lk

D.Y. Mudunkotuwa
Department of Mechanical Engineering
Faculty of Engineering
University of Sri Jayewardenepura
Rathmalana, Sri Lanka
Dulini@sjp.ac.lk

Abstract— **Noise generation from aircrafts has become a major problem in the current aviation industry. As a solution, scientists have conducted variety of research studies by modifying the wings with three main features of owl species which allow them to fly in silent. Those are leading edge serrations, trailing edge serrations and the porosity on the wings. Due to the increase of drag from porous designs, most of the flow generated noise reduction aimed research studies have conducted by applying leading edge serrations and trailing edge serrations. Though, there were no research performed by adding both leading edge serrations as well as trailing edge serrations on an airfoil implemented wing. Therefore, this research was conducted by modifying a NACA 0012 airfoil type wing by adding both leading edge serrations as well as trailing edge serrations. At first, this research considered the highest noise reduced leading edge and trailing edge serration geometries from literature and modified the NACA 0012 base wing. Then, the research considered the main three types of leading-edge serration geometries of one of a highest noise reducing owl species in the world called A. Otus owl and modified the NACA 0012 base wing using the serration geometries of their wing. The acoustic simulations were conducted along with the aerodynamic simulations to configure the noise reduction as well as the change in aerodynamics of the wing with different serration geometries. Finally, the highest noise reducing serration geometries and the lowest aerodynamic properties changing serration geometries were identified.**

Keywords— aerodynamic, airfoil noise reduction, biomimicry, bioinspired airfoil

I. Introduction

Rapid development in the aviation industry have increased the popularity in air travelling which led to increase the number of large aircrafts. For manage that higher number of aircrafts, more expanded airports have been increased which created the aircraft noise a major problem. Therefore, the International Civil Aviation Organization has set many strict regulations for the aircrafts. In aircrafts, two types of noises are generated by engines and by airframe. For reduce the aircraft noise in the early era, the main focus was on the noise from the engine. When engine noise had significantly reduced through various improvements in past decades, the focus went to the improvement of aircraft wings. One of a key area of this modification was using biological inspirations from different types of birds which have the ability to fly in silent. Specially, many owl species have the ability to fly in silent. Barn owl is one of an owl species that has this ability. This is mainly caused by the special feather adaptations of them. The study [1] has identified three unique characteristics in owl feathers which reduce the flight noise of them when comparing the feathers of owl's and non-silent flying birds. Those are the trailing edge serrations, leading edge serrations and the downy coat on flight feathers. By inspired from those unique characteristics, many research studies have been conducted in the purpose of reducing the aircraft wing noise.

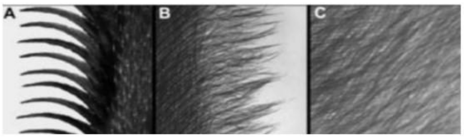

Fig. 1. Leading edge serrations, trailing edge serrations and downy coat in Barn owl flight feathers [2].

II. Literature Survey

A. Actual leading edge serration geometries of owl feathers

The research [3] investigated serrations of seven types of owl species. When choosing the owl species, their selection criteria was to consider different sized owls as well as owls with different activity patterns. They selected two large owl species whose body weight was higher than 1kg (Bubo, Scandiacus), three middle sized owl species whose body weight was in between 0.3kg and 1kg (T. Furcata Pratincola, A. Otus, A. Flammeus), two small sized owl species whose body weight was below 0.3kg (A. Funereus, A. Noctua). According to the previous research studies, the owl leading edge serrations were only present at the 10th primary section of the owl wing leading edge as follows.

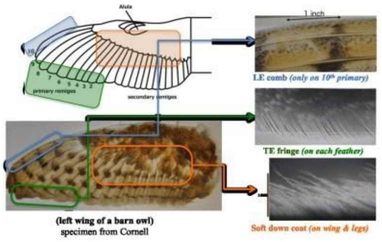

Fig. 2. The sections of a barn owl wing that have the noise reduction mechanisms [3]

III. Methodology

A. Computational Fluid Dynamics (CFD)

Computational fluid dynamics is used in fluid mechanics to analyze the behaviors of fluid flows in various applications. CFD models the fluid as a continuous medium and the behaviors of the fluid is described using a set of governing equations which vary according to the mathematical model that use for the calculations. For this study, a commercially available CFD software called ANSYS Fluent has been used due to its variety of advantages such as high accuracy in results, ability to efficiently handle even large-scale simulations with parallel computing and the user-friendly interface, etc.

B. Verifying the numerical models with experimental analysis

1) K-epsilon model.

The k-epsilon realizable model with two equations was chosen as the viscous model. This is due to the reason that the k-epsilon uses less computing power than the models with more equations. Also, the k-epsilon model is accurate enough for turbulent models as well as this model belonged to the Reynold's Average Navier-Stokes equation family and it solve the Navier Stokes equation numerically.

The two transport equations which uses in k-epsilon model is as below.

a) Transport equation for turbulent kinetic energy (k).

This equation explains how the turbulent kinetic energy in a flow is produced, diffused, and dissipated. This equation is solved for the turbulent kinetic energy per unit mass, k.

$$\frac{\partial}{\partial t}(\rho k)+\frac{\partial}{\partial x_j}(\rho k u_j)=\frac{\partial}{\partial x_j}\left[\left(\mu+\frac{\mu_t}{\sigma_k}\right)\frac{\partial k}{\partial x_j}\right]+G_k+G_b-\rho\epsilon-Y_M+S_k \tag{1}$$

b) Transport equation for the rate of dissipation of turbulent kinetic energy (epsilon).

This equation describes how the turbulent kinetic energy dissipation happens due to the viscosity of the fluid. This equation is solved for the rate of dissipation per unit mass, epsilon.

$$\frac{\partial}{\partial t}(\rho\epsilon)+\frac{\partial}{\partial x_j}(\rho\epsilon u_j)=\frac{\partial}{\partial x_j}\left[\left(\mu+\frac{\mu_t}{\sigma_\epsilon}\right)\frac{\partial \epsilon}{\partial x_j}\right]+\rho C_1 S\epsilon-\rho C_2\frac{\epsilon^2}{k+\sqrt{\nu\epsilon}}+C_{1\epsilon}\frac{\epsilon}{k}C_{3\epsilon}G_b+S_\epsilon \tag{2}$$

u_j= Velocity component in corresponding direction

G_k = Generation of turbulence kinetic energy due to the mean velocity gradients

G_b = Generation of turbulence kinetic energy due to the buoyancy

Y_M= Fluctuating dilatation in compressible turbulence

μ_t= Eddy viscosity

C_2, $C_{1\varepsilon}$= Constants

σ_k, σ_ϵ= turbulent Prandtl numbers

2) Ffowcs Williams and Hawkings (FW-H) model.

The Ffowcs Williams and Hawkings (FW-H) model is used to predict the sound that produce from unsteady fluid flows. The Ffowcs Williams and Hawkings (FW-H) equation is a generalized form of Lighthill acoustic analogy which relate the changing fluid pressure to the sound waves that radiate from a turbulent flow.

3) Lighthill acoustic analogy.

Sir James Lighthill have created a general equation for aeroacoustic problems using the derivations from Navier-Stokes equations,.

$$\frac{\partial^2\rho}{\partial t^2}-c_0^2\nabla^2\rho=\frac{\partial^2 T_{ij}}{\partial x_i\partial x_j} \tag{3}$$

T_{ij} = Lighthill's stress tensor

By manipulating the conservation equations, following FWH model has been created.

$$\frac{1}{a_0^2}\frac{\partial^2\rho'}{\partial t^2}-\nabla^2\rho'=\frac{\partial^2}{\partial x_i\partial x_j}\{T_{ij}H(f)\}-\frac{\partial}{\partial x_i}\{[P_{ij}n_j+\rho u_i(u_n-v_n)]\delta(f)\}+\frac{\partial}{\partial_i}\{[\rho_0 v_n+\rho(u_n-v_n)]\delta(f)\} \tag{4}$$

u_i= fluid velocity component in the x_i direction

u_n= fluid velocity component normal to the surface

v_i= surface velocity component in the x_i direction

v_n= surface velocity component normal to the surface

$\delta(f)$= Dirac delta function

$H(f)$= Heaviside function

ρ'= Sound pressure at the far field

a_0= Far field sound speed

P_{ij}= Compressive stress tensor

n_j= Unit normal vector

4) Verification of mathematical model.

The mathematical model was verified using a NACA 0012 wing with 150mm chord length. The simulations were performed for the 292,397 Reynolds number with 9 degrees Angle of attack.

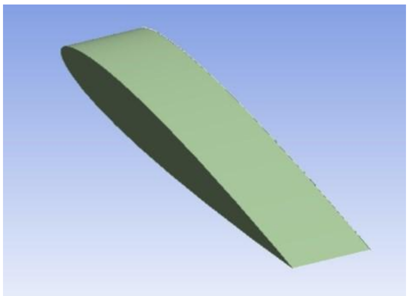

Fig. 3. Base NACA 0012 wing

The computational domain was created using Ansys.

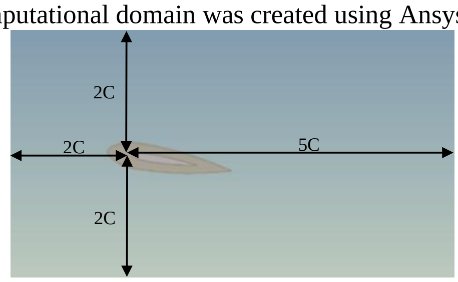

Fig. 4. Computational domain

The boundary conditions were set as follows

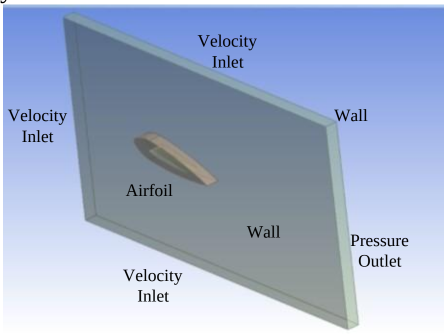

Fig. 5. Boundary conditions the simulation

This study simulated a NACA 0012 airfoil using an unstructured mesh.

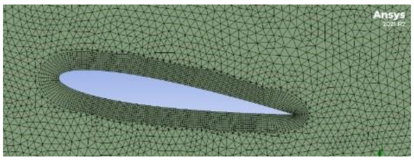

Fig. 6. Mesh near to the wing

In the mesh, the largest element size was 5 mm and it was near the walls and the smallest element was 1mm and it was near the airfoil. The total number of elements were 1,249,821.

Following parameters were used for the calculations:
Fluid density = 1.225 kg/m^3
Temperature = 288.16K
Viscosity = 1.7894e-05 kgm^{-1}s^{-1}
Velocity = 20 ms^{-1}
Chord length = 150mm
Span = 37.5mm
Angle of Attack = 9°

Receiver placement,
The acoustic receivers were defined and placed according to the FW-H method. Receivers were placed in the upper face of the domain parallel to the trailing edge as follows.

Fig. 26. Acoustic receiver placement in the simulation

5) Verification of the acoustic model.

For verify the acoustic model of the simulation, the experimental acoustic data of study [4] was used. The [4] research has done the experiment for the Reynolds number of 292,397 with 150mm chord length and 9° Angle of Attack. In this simulation, the same computational domain and the same mesh was used with Ffowcs Williams and Hawkings (FW-H) model.

C. Analysis 1: Simulation for airfoil noise reduction using highest noise reduced leading edge serration geometry from literature.

From literature [5], the highest noise reduction was occurred for the leading edge serration geometry of 15mm Amplitude and 15mm Wavelength. In this analysis, the leading edge serrations as well as the trailing edge serrations of NACA 0012 wing were designed from SolidWorks using the serration geometry. This serration geometry will be mentioned as A10W10 serrations in the following analysis. The chord length of the wing was 150mm and the angle of attack was 9 degrees. Following are the parameters of the serrations,
Serration amplitude = 0.1c
= 15mm
Serration wavelength = 0.1c
= 15mm

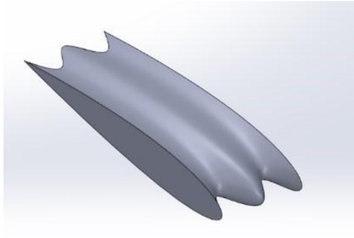

Fig. 7. Modified NACA 0012 wing with A10W10 serrations

D. Analysis 2: Simulation for airfoil noise reduction using the highest noise reduced trailing edge serration geometry from literature.

From literature [6], the highest noise reduction was occurred for the trailing edge serrations from the serration geometry of 20mm Amplitude and 4.9mm Wavelength. In this analysis, the leading-edge serrations as well as trailing edge serrations of NACA 0012 wing were designed according this geometry and this serration geometry will be mentioned as S1 serrations in the following analysis.

Following are the parameters of the serrations,
Serration amplitude = 20 mm
Serration wavelength = 4.9mm

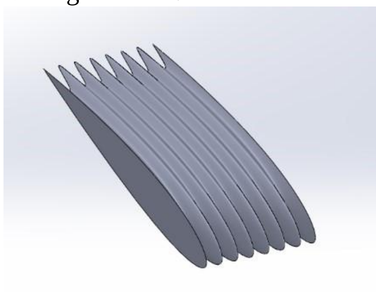

Fig. 8. Modified NACA 0012 wing with S1 Serrations

E. Analysis 3: Simulation for the airfoil noise reduction using leading edge serration geometries of actual owl wing.

As mentioned in the literature survey, in research [3], the 10th primary section feathers were divided into mainly 4 sections and investigated the differences in serrations in each section. A feather in a 10th primary section with the serration geometries of A. Otus owl species was named as follows.

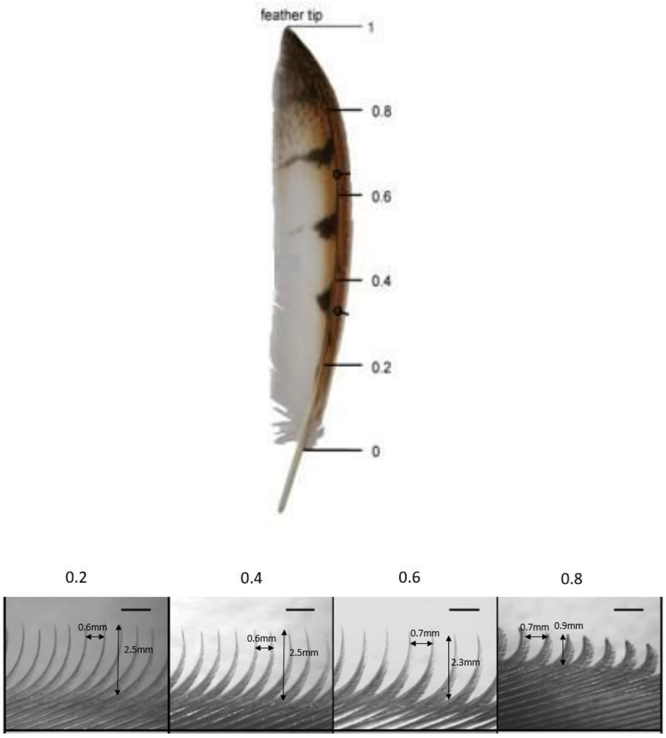

Fig. 9. Sections of an owl feather at 10th primary section [3]

The 0.2 and 0.4 sections have almost same leading edge serration geometry with the amplitude of 2.5mm and the wavelength of 0.6mm. The leading-edge serrations at 0.6 section of the leading edge had 2.3mm amplitude and 0.7mm wavelength. The leading-edge serrations at 0.8 section had the amplitude of 0.9mm and 0.7mm wavelength. In this analysis, the NACA 0012 wing was modified with the main three Amplitude/wavelength ratios of the different sections of owl's leading edge.

In this analysis, the leading edge serration geometry at 0.2 and 0.4 sections was defined as Owl A and the serration geometries at 0.6 and 0.8 sections were defined as Owl B and Owl C correspondently.

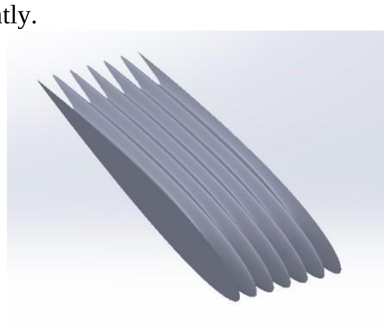

Fig. 10. Modified NACA 0012 wing with Owl A type serrations

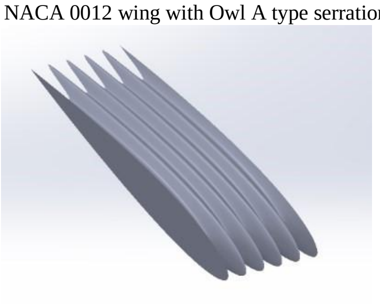

Fig. 11. Modified NACA 0012 wing with Owl B type serrations

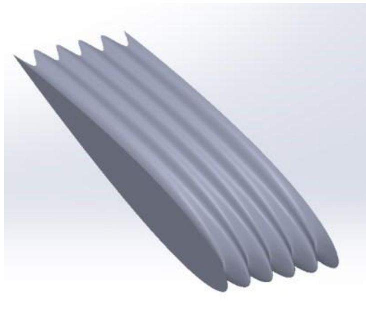

Fig. 12. Modified NACA 0012 wing with Owl C type serrations

F. *Mathematical model verification*

Results for the simulation of NACA 0012 airfoil with 150mm chord length and 37.5mm span with 9° angle of attack are as follows.

TABLE I. COMPARISON OF SIMULATION RESULTS WITH EXPERIMETAL RESULTS

	Simulation	Experimental
Lift coefficient	0.719	0.76
Drag coefficient	0.063	0.06

The experimental results of the research [4] and the performed simulation results had 6.5% difference. Therefore, the mesh parameters were taken as a suitable mesh for this study.

G. *Verification of the acoustic model*

Following graph shows the acoustic results of the experiment [4] and the acoustic simulation results for the unmodified NACA 0012 wing with 150mm chord length.

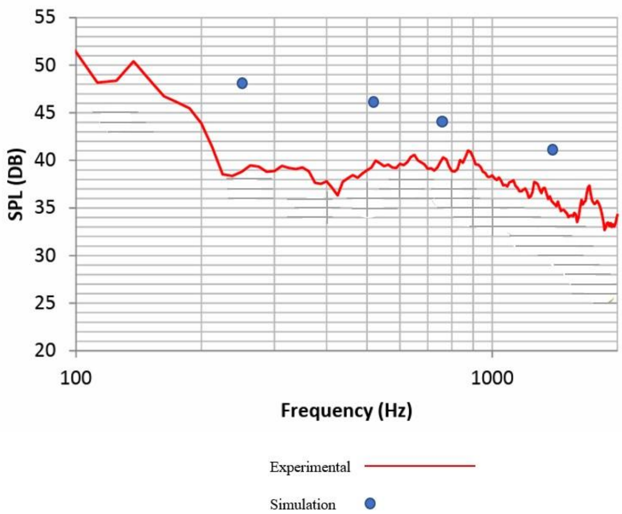

Fig. 13. Comparison of the acoustic measurements of experimental and simulation results [4]

As the sound pressure levels in the simulation was closer to the experimental results, the acoustic setup which used for the above simulation was taken as a suitable setup for this study.

IV. RESULTS AND DISCUSSION

A. Results of Analysis 1

TABLE II. COMPARISON OF AERODYNAMIC COEFFICIENTS OF A10W10 SERRATED WING WITH BASE WING

	Lift coefficient	Drag coefficient
Base wing	0.719	0.063
A10W10 serrated wing	0.558	0.061

The A10W10 serrations didn't affect for the drag coefficient value thoroughly. However, it has reduced the lift coefficient value of the base wing.

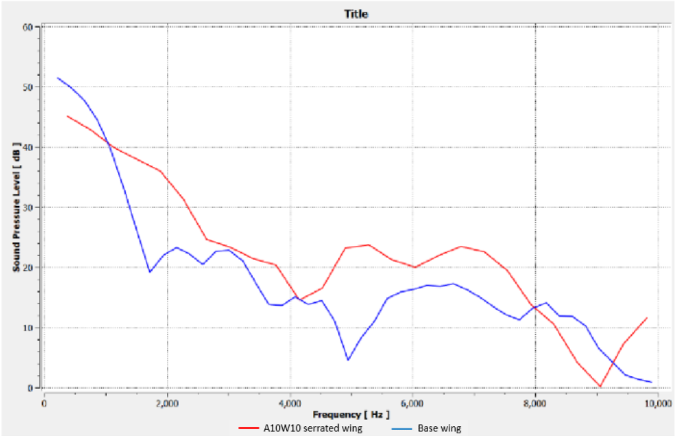

Fig. 14. Comparison of the acoustic measurements of A10W10 serrated wing with base wing

The A10W10 serration type has significantly reduced the noise generation in 0 Hz to 1000Hz frequency range.

B. Results of Analysis 2

TABLE III. COMPARISON OF AERODYNAMIC COEFFICIENTS OF S1 SERRATED WING WITH BASE WING

	Lift coefficient	Drag coefficient
Base wing	0.719	0.063
S1 serrated wing	0.551	0.103

The S1 type serrations have reduced the lift coefficient of the base wing and significantly increased the drag coefficient value of the base wing.

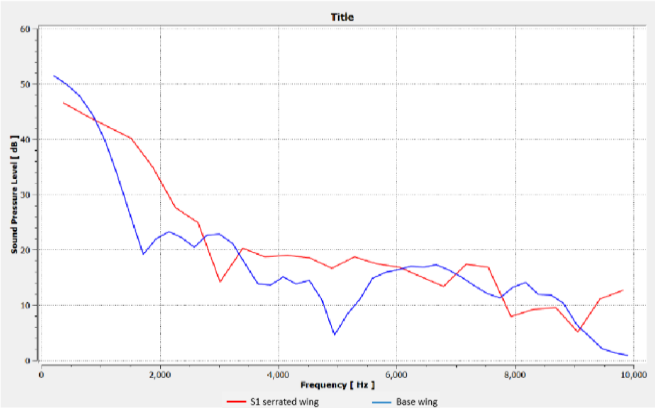

Fig. 15. Comparison of acoustic measurements of S1 serrated wing with base wing

The S1 type serrations have significantly reduced the noise generation in 0 Hz to 1000 Hz frequency range.

C. Results of Analysis 3

TABLE IV. COMPARISON OF AERODYNAMIC COEFFICIENTS OF OWL A TYPE, OWL B TYPE AND OWL C TYPE SERRATED WINGS WITH BASE WING

	Lift coefficient	Drag coefficient
Base wing	0.719	0.063
Owl A type	0.475	0.101
Owl B type	0.484	0.088
Owl C type	0.539	0.067

The lift coefficient of the base wing has reduced by all the above serration types and the drag coefficient of the base wing has increased by all the above serration types. The Owl A type serrations have significantly increased the drag coefficient of the base wing.

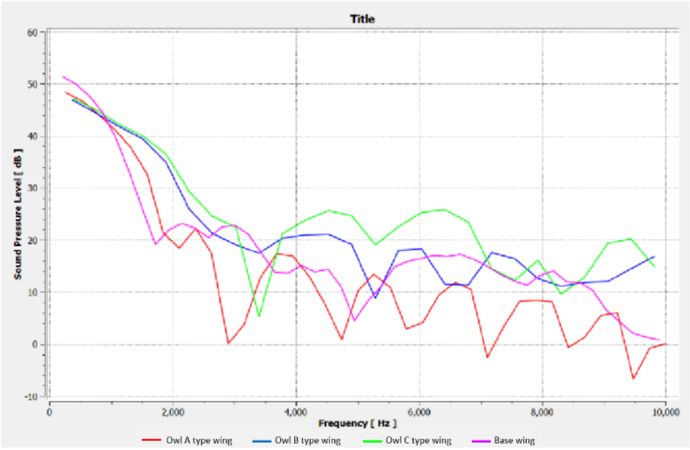

Fig. 16. Comparison of acoustic measurements of Owl A, B and C type serrated wings with base wing

The Owl B type serrations reduced the 0 Hz to 1000Hz frequency range noise in the highest level. The Owl A serration type is the highest overall noise reduced serration type, when consider the frequency range after 1000Hz.

D. Comparison of all serration types

1) Comparison of the aerodynamic coefficients.

TABLE V. COMPARISON OF AERODYNAMIC COEFFICIENTS OF ALL THE SERRATED WINGS WITH BASE WING

	Lift coefficient	Drag coefficient
Base wing	0.719	0.063
A10W10	0.558	0.061
S1	0.551	0.103
Owl A	0.475	0.101
Owl B	0.484	0.088
Owl C	0.539	0.067

All the serration types have reduced the lift coefficient of the base wing and increased the drag coefficient of the base wing other than A10W10 serration type which reduced the drag coefficient of the base wing. The highest drag coefficients were generated by the S1 type and the Owl A type serrations. When the wavelength of the serrations were increased, the drag coefficient was decreased and the lift coefficient was increased.

2) Comparison of the acoustic measurements.

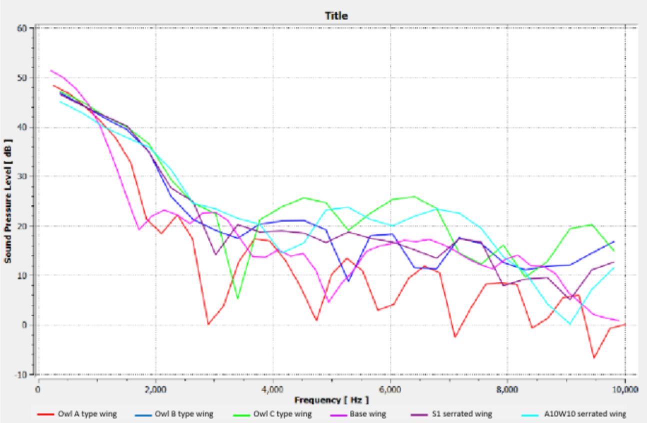

Fig. 17. Comparison of acoustic measurements of all serration types

The A10W10 serration type was the highest 0 Hz to 1000Hz noise reduced serration type. The Owl A serration type was the highest overall noise reduced serration type when consider the frequency range after 1000Hz.

Therefore, if consider about noise reduction, the best Amplitude/ Wavelength ratio would be 2mm/4mm which used in the Owl A type serrations. If consider about the change in the aerodynamics, the best Amplitude/ Wavelength ratio would be 15mm/15mm which used in A10W10 serrations.

V. CONCLUSION

As the first step of this research, the mathematical models were validated using the experimental results of the research [4] using a NACA 0012 base wing with 150mm chord length. Then the NACA 0012 wing was modified by adding highest noise reduced leading edge serration geometry of the study [5] on both edges of the base wing (on leading edge as well as on the trailing edge). Then the same base wing was modified by adding highest noise reduced trailing edge serration geometry of the study [6] on both edges of the base wing. After investigating the leading edge serration geometries of different owl species in the world, the A. Otus owl was chosen to get the serration geometries as that owl has a significant noise reducing ability when compared to other owl species. Then the NACA 0012 base wing was modified by applying the main leading edge serration geometries of A. Otus owl species to the both leading edge as well to the trailing edge. The acoustic simulations were conducted for each and every modified wing and investigated how the noise generation was varying according to the particular serration geometries. When consider about the acoustic simulations results, the A10W10 serration type was the highest 0Hz to 1000Hz noise reduced serration type and the Owl A serration type was the highest overall noise reduced serration type. Then the research considered about the change of aerodynamics when adding the same serrations to the base wing. According to the results of the simulations, when the serration wavelength was increased, the drag coefficient was decreased and the lift coefficient was increased. Therefore, the A10W10 serration type had the highest lift coefficient and the lowest drag coefficient when compared to the other serration types. In the aircrafts, as the drag need to be reduced as high as possible as well as lift need to be increased as high as possible, the serration wavelength must be limited when selecting a serration type for implement on the actual aircraft wings to reduce the aircraft noise.

VI. FUTURE WORKS

This research can be continued by modifying NACA 0012 base wing by adding different leading edge serration geometries and different trailing edge serration geometries on the same wing.

REFERENCES

[1] R. R. Graham, “The silent flight of owls,” The Journal of the Royal Aeronautical Society, vol. 38, no. 286, pp. 837–843, 1934.

[2] G. Lilley, “A study of The silent flight of the owl,” 4th AIAA/CEAS Aeroacoustics Conference, 1998.

[3] M. Weger and H. Wagner, “Morphological variations of leading-edge serrations in owls (strigiformes),” *PLOS ONE*, vol. 11, no. 3, 2016. doi:10.1371/journal.pone.0149236

[4] D. Y. MUDUNKOTUWA, “LES of airfoil flows by using voxel mesh ,” *LES of airfoil flows by using voxel mesh*, pp. 2–55, Feb. 2013

[5] A. S. Hersh, P. T. Soderman, and R. E. Hayden, “ Acoustic investigation of leading-edge serrations on lifting surfaces,” The Journal of the Acoustical Society of America, vol. 50, no. 1A, pp. 121– 121, 1971

[6] M. Gruber, M. Azarpeyvand, and P. F. Joseph, “Airfoil trailing edge noise reduction by the introduction of sawtooth and slitted trailing edge geometries,” no. 2010, pp. 1–9, Aug. 2010.

[7] Y. Wang, K. Zhao, X.-Y. Lu, Y.-B. Song, and G. J. Bennett, “Bioinspired aerodynamic noise control” Applied Sciences, vol. 9, no. 11, p. 2224, 2019.

[8] C. C. Paruchuri, S. Narayanan, P. Joseph, and J. W. Kim, “Leading edge serration geometries for significantly enhanced leading edge noise reductions,” 22nd AIAA/CEAS Aeroacoustics Conference, 2016.

[9] G. M. LILLEY, “The prediction of airframe noise and comparison with experiment,” Journal of Sound and Vibration, vol. 239, no. 4, pp. 849– 859, 2001

[10] G. Lacagnina et al., "Leading edge serrations for the reduction of aerofoil self-noise at low angle of attack, pre-stall and post-stall conditions", International Journal of Aeroacoustics, vol. 20, no. 1-2, pp. 130-156, 2021. Available: 10.1177/1475472x20978379.

[11] M. Gruber, P. Joseph, and T. P. Chong, “Experimental investigation of airfoil self noise and turbulent wake reduction by the use of trailing edge serrations,” 16th AIAA/CEAS Aeroacoustics Conference, 2010.

[12] M. Gruber, P. Joseph, and T. Chong, “On the mechanisms of serrated airfoil trailing edge noise reduction,” 17th AIAA/CEAS Aeroacoustics Conference (32nd AIAA Aeroacoustics Conference), 2011

[13] T. P. Chong, P. Joseph, and M. Gruber, “An experimental study of airfoil instability noise with trailing edge serrations,” 16th AIAA/CEAS Aeroacoustics Conference, 2010.

[14] T. P. Chong, P. Joseph, A. Vathylakis, and M. Gruber, “On the noise and wake flow of an airfoil with broken and serrated trailing edges,” 17th AIAA/CEAS Aeroacoustics Conference (32nd AIAA Aeroacoustics Conference), 2011.

[15] M. S. Howe, “Aerodynamic noise of a serrated trailing edge,” Journal of Fluids and Structures, vol. 5, no. 1, pp. 33–45, 1991.

[16] C. C. Paruchuri, S. Narayanan, P. Joseph, and J. W. Kim, “Leading edge serration geometries for significantly enhanced leading edge noise reductions,” 22nd AIAA/CEAS Aeroacoustics Conference, 2016.